Advances in Thermal Processes and Energy Transformation
Volume 7, 2024, KIZE04, pp.10-18, ISSN 2585-9102
https://doi.org/10.54570/atpet2024/07/01/0010

Analysis of Pressure Losses in Experimental Devices for Measuring Small Gas Flows Using CFD Modelling

Ján Kizek[1] ● Róbert Dzurňák [2] ● Marcel Fedák[1] ● Augustín Varga[2] ● Denys Zhumar[3]

[1]Technical University of Košice, Faculty of Manufacturing Technologies with a seat in Prešov, Department of Process Technique, Bayerova 1, 080 01 Prešov, Slovak Republic, jan.kizek@tuke.sk, marcel.fedak@tuke.sk
[2]Technical University of Košice, Faculty of Materials, Metallurgy and Recycling, Institute of Metallurgy, Letná 9, 042 00 Košice, Slovak Republic, robert.dzurnak@tuke.sk, augustin.varga@tuke.sk
[3]Oles Honchar Dnipro National University, Physical and technical faculty, Gagarina Avenue 72, Dnipro, 49010, Ukraine, zhumar82@gmail.com

Category : Original Scientific Paper
Received : 21 March 2024 / Revised: 28 March 2024 / Accepted: 29 March 2024

Keywords: CFD model, experimental device, pressure loss, small gas flow

Abstract: In the paper, the authors analysed pressure losses on experimental devices for measuring small flows of gaseous media using CFD modelling. The visualization of the obtained results using CFD models for 3 experimental devices illustrates the pressure profiles for these devices. The created CFD models compare different principles of creating pressure loss on created devices. From the analysis of pressure profiles, it is possible to observe the tendencies of pressure decreases along the length of experimental devices for measuring small flows. Modelling results can be used for possible modifications of experimental equipment.

Citation: Kizek Ján, Dzurňák Róbert, Fedák Marcel, Varga Augustín, Zhumar Denys: Analysis of Pressure Losses in Experimental Devices for Measuring Small Gas Flows Using CFD Modelling, Advance in Thermal Processes and Energy Transformation, Volume 7, No.1 (2024), pp. 10-18, ISSN 2585-9102, https://doi.org/10.54570/atpet2024/07/01/0010.

1 Introduction

As it has already been mentioned in many publications and on professional forums, gas flow measurement is very important for both customers and suppliers due to the correct evaluation of consumption, and production, but especially the supply of a given amount of gas.

For a correct understanding of this issue, it is necessary to know the regularities of the properties of the flowing medium as well as the characteristics of the measuring devices when measuring gas quantities. In [1, 2], the authors address the basic characteristics of gas flow for a better understanding, where the importance of determining the flow regime is explained. The flow mode is also important for the accuracy of determining the flow of gas through a monitored element or through the cross-section of a pipe or channel. This is all the more important for determining low gas flows. It is considered that for such low flow rates, it is advisable to use the laminar flow mode. The differences between laminar and turbulent flow regimes are explained clearly in [3].

In publications [4-9], the authors explained in detail the principles of flow measurements using various measuring devices. The described measuring devices are based on flow measurement based on various physical principles. The appropriateness of the use of the given measuring devices is determined from these applied principles. A device based on the principle of laminarization of flow along the length of the measuring elements (capillaries) appears to be a very interesting device for measuring low flow rates. This issue is explained in [4] and its application is also detailed in [10-12], where the authors take a closer look at commercially produced measuring devices known as Laminar flow elements.

The authors present the problem of flow with visualization and software simulation in [13-14]. In the publication [13], the bubble method, which is used to determine critical points, was used to visualize the flow in an experimental device or in a transparent pipe.

Knowledge from the mentioned publications was used in the design of experimental devices, which are described in detail in [15] for the design of experimental devices No.1 and No.2 based on the principle of local pressure loss and in [16] experimental device No.3 based on the principle of laminarization of flow in the measuring element composed of capillaries.

The authors in the presented article aim to use modelling in CFD software to visualize the pressure decrease along the length of the measuring element for two gaseous media, namely air and natural gas, the composition of which was taken from [17]. The created simulations are based on experimental measurements for specific flow rates, which are presented in [15] and [16].

2 Materials and methods

The creation of simulation models is based on actual devices, where experimental measurements determine the behaviour of selected parameters on the developed physical models or experimental devices. For the visualization of the chosen parameters, the method of flow simulation in the designed experimental devices using CFD simulation software was selected. In this case, the ANSYS R16.2 software was used. For the visualization of the pressure field, the Colour Contour method was chosen to distinguish pressure magnitude.

2.1 CFD model-experimental devices

The created CFD models are based on the design of three experimental devices for measuring small flow rates, which are described in detail in [15] and [16]. In [15], the devices for CFD models that generate pressure loss based on the principle of local pressure loss due to an obstacle are described.

The calculations of pressure losses were based on the following mathematical relationship for determining the local pressure loss coefficient, [1]:

$$\Delta p = \xi \frac{w_t^2}{2} * \rho_t \qquad (1)$$

ξ - the calculated local pressure loss coefficient, (-),
Δp - pressure difference at the device, (Pa),
ρ_t - density of the flowing medium at the measured pressure and temperature, (kg.m^{-3}),
w_t - the actual velocity of the fluid flow, at the measured pressure and temperature, (m.s^{-1}).

In [16], the third experimental device for the created CFD model is described, which models pressure loss along the length of the measuring device based on the principle of flow laminarization in a capillary system. In this case, the created model generates pressure loss along the length of the capillaries in the measuring element. For reasons described in [15] and [16], the measuring element was considered a local obstacle, and the calculation of pressure loss was conducted similarly to the first and second experimental devices using the mathematical relationship (1).

The mathematical model for the experimental device was created in Ansys Fluent. The basis of the model was the description of flow through the Navier-Stokes equation, supplemented by the passage of the medium through a porous layer (wire mesh), which was defined using Darcy's law. Darcy's law is an essential tool in the analysis of fluid flow through porous media, used in various engineering applications, and is defined as follows:

$$Q = -kA\frac{dp}{dx} \qquad (2)$$

Q - the volumetric flow rate of the fluid, (m³.s^{-1}),
k - the permeability of the porous medium, (m²),
A - the cross-sectional area of the medium perpendicular to the flow direction, (m²),
dp/dx - the pressure gradient along the flow direction, (Pa.m^{-1}).

This law states that the volumetric flow rate of the fluid is directly proportional to the permeability k, the cross-sectional area A, and the pressure gradient dp/dx in the direction of fluid flow. The negative sign indicates that the flow will move from a region of higher pressure to a region of lower pressure.

In the field of CFD modelling, the Brinkman equation is used to model flow through porous regions. This equation is a modified form of the Navier-Stokes equation that accounts for the resistance within the medium. The Brinkman equation is essential for modelling fluid flow in environments with varying permeabilities and porosities. It is defined by the following relationship:

$$\rho\left(\frac{\partial u}{\partial t} + u\,.\,\nabla u\right) = -\nabla p + \mu\nabla^2 u - \frac{\mu}{\varepsilon^2 u} \qquad (3)$$

ρ - the fluid density, (kg.m^{-3}),
u - the velocity vector, (m.s^{-1}),
p - the pressure, (Pa),
μ - the dynamic viscosity, (Pa·s),
ε - characteristic dimension related to the porosity and permeability of the medium, (m).

The boundary conditions on the input side of the mathematical model were defined based on the volumetric flow rates and input pressures recorded during experimental measurements, as specified in [15] for experimental devices No.1 and No.2, and in [16] for experimental device No.3.

3 Results and discussion

3.1 Experimental device No.1

The created CFD model for experimental device No.1 was based on the first experimental device described in [15]. In the simulation, a specific gas flow rate and the measured pressure at the beginning of the

experimental device were set. Another parameter was derived from the filler, which created resistance to the flow and thus generated a pressure decrease at the location of the filler. Since the wire mesh used as the filler in the experimental device is difficult to define precisely, the filler in the model was defined as a porous material. Air and natural gas from the distribution pipeline were used as the gaseous media. The composition of natural gas from [17] was used to set the physical parameters and properties of the gas.

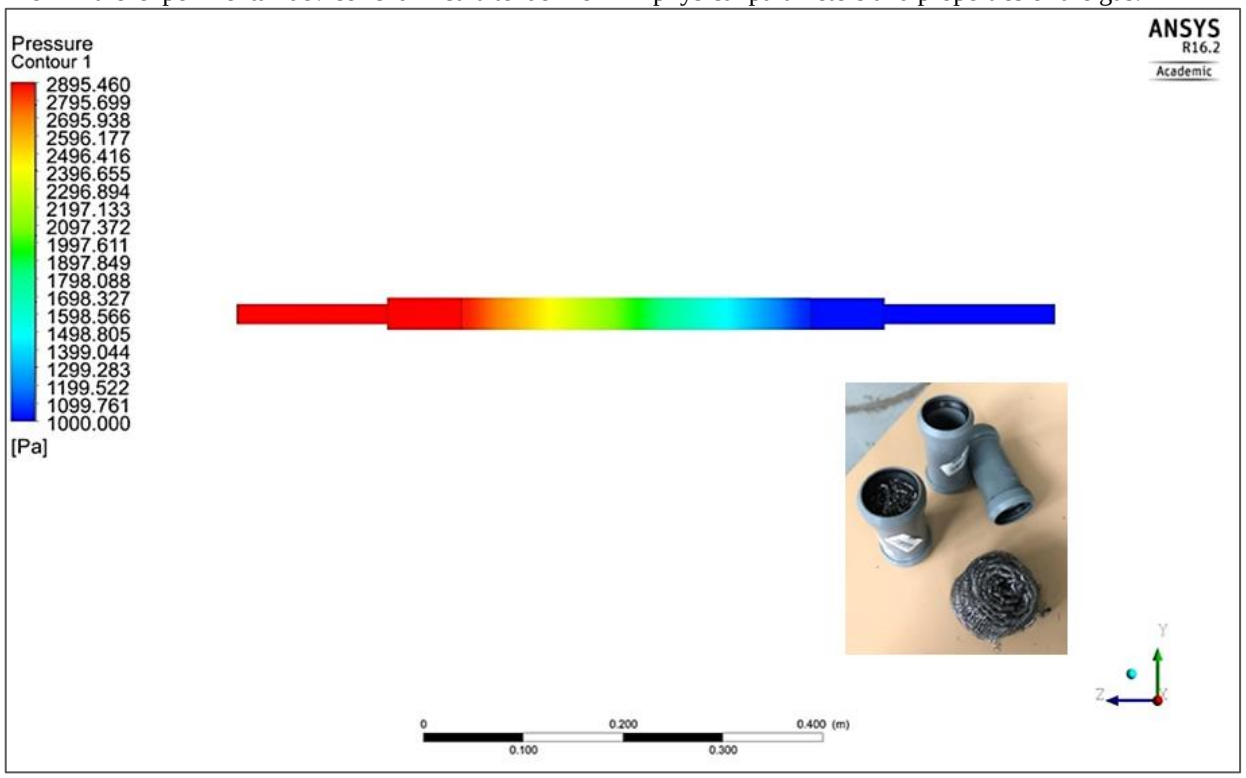

Figure 1 Simulation of the pressure field in experimental model No.1 for air flow 4746.79 $l.h^{-1}$

In Figure 1, the result of the flow simulation in Model No.1 for the air flow rate q_{v0} = *4746.79* $l.h^{-1}$ and the input pressure from Table 1 in [15] is shown. The visual representation of the pressure field along the length of the measuring element is depicted using a colour contour. From the analysis of the pressure field, a smooth pressure gradient can be observed at the filling location using kitchen wire.

In Figure 2, the pressure decrease along the length of the measuring element is shown using a curve, which indicates a smooth pressure decrease at the filling location. For simulations in CFD software, this material was defined as a porous material, and therefore, it can be inferred that the shape of the curve and the pressure decrease can be influenced by defining the pore size at the filling location. For the experimental setup, this means that the pressure loss coefficient is dependent on the quantity or density of the filling using kitchen wire.

From the analysis of the pressure profile along the length of the measuring element for the set flow rate and initial pressure, a pressure decrease of *1895 Pa* was obtained using CFD simulation. The shape of the curve shows the length of the section where the filling was located, which was *35 cm* long. A smooth pressure decrease can be observed along the entire length of the filling. The CFD software simulation suggests uniform flow distribution along the entire length of the filling. Due to the complex geometry of the kitchen wire used as the filling, estimating the parameters of the porous filling defined in the software is complicated.

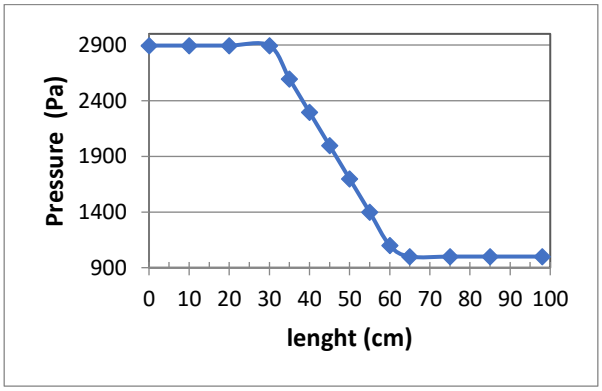

Figure 2 Pressure decrease along the length of the No.1 model for CFD flow simulation – Air

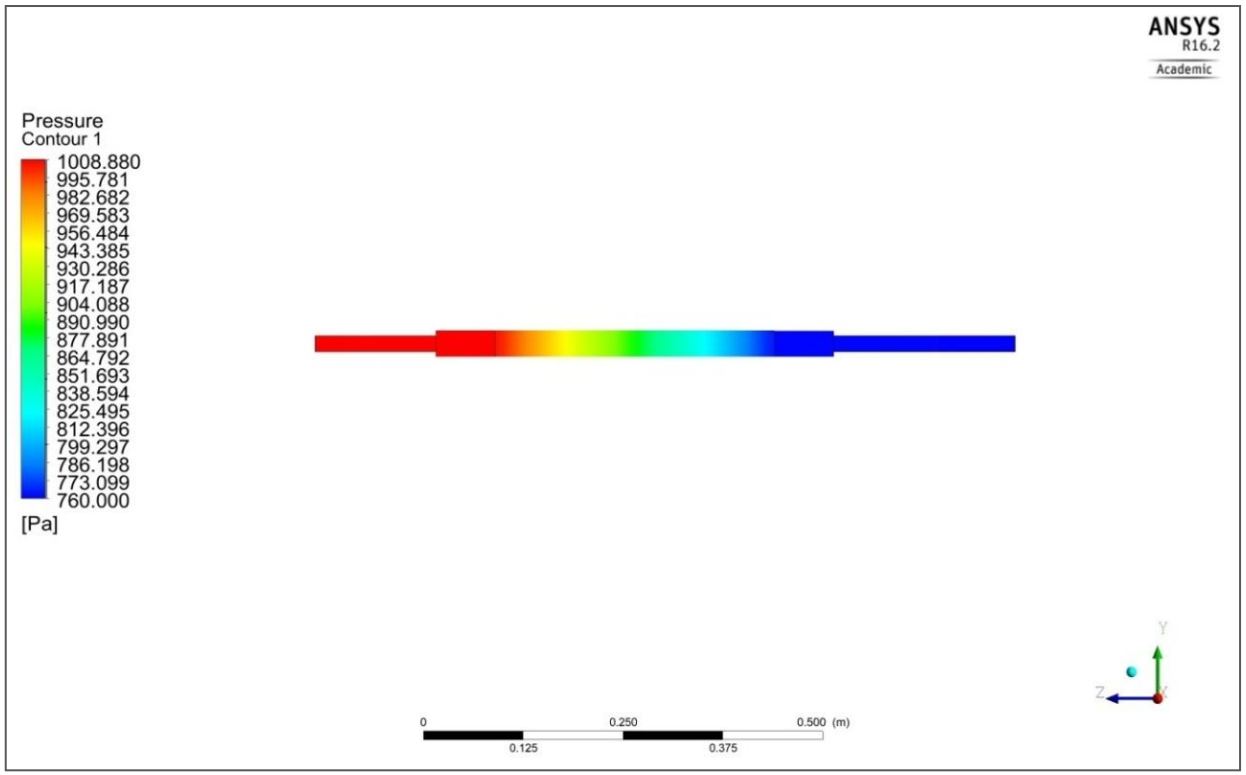

Figure 3 Simulation of the pressure field in experimental model No.1 for natural gas flow 1297.18 $l.h^{-1}$

In Figure 3, the result of the flow simulation in Model No.1 for the natural gas flow rate $q_{v0} = 1297.18\ l.h^{-1}$ from Table 2 in [15] is shown. The visual representation of the pressure field along the length of the measuring element is depicted using a colour contour. From the analysis of the pressure field, a smooth pressure gradient can also be observed at the filling location using kitchen wire.

In Figure 4, the pressure decrease along the length of the measuring element is shown using a curve, which indicates a smooth pressure decrease at the filling location. For the CFD software simulations, the geometry parameters were set similarly to the case of air flow, and this material was defined as a porous material. Natural gas, as the gaseous medium used, exhibits different physical properties compared to air, resulting in a lower pressure decrease than when air is used as the gaseous medium. From the analysis of the pressure profile along the length of the measuring element for the set flow rate and initial pressure, a pressure decrease of *248 Pa* was obtained using CFD simulation. Again, a smooth pressure decrease can be visually observed due to the change in flow characteristics through the defined porous filling of the measuring element.

The experimental measurements yielded different pressure decrease values due to the simplified geometry of the measuring element's filling and the difficulty of defining the geometry of the kitchen wire. The mentioned filling creates a network of various channels that do not have the same geometry, and their diversity would require a high level of detail to accurately create such geometry.

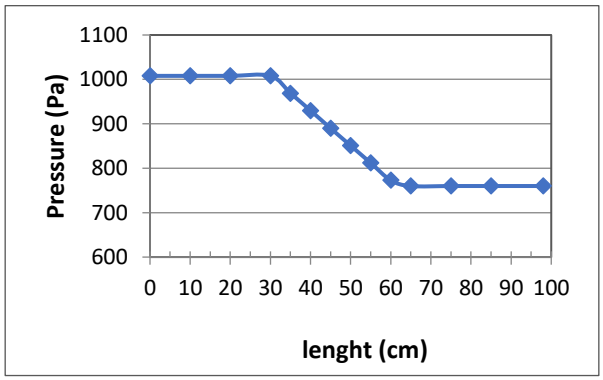

Figure 4 Pressure decrease along the length of the No.1 model for CFD flow simulation – Natural gas

3.2 Experimental device No.2

The created CFD model for experimental device No.2 was based on the second experimental apparatus described in [15]. In the simulation, a single gaseous medium flow rate and the measured pressure at the beginning of the experimental device were set.

Another parameter was derived from the filling, which consisted of three siphon strainers acting as a local obstacle to the flow and causing a local pressure decrease. The geometry of the siphon strainers is of a simpler design compared to the filling in experimental device No.1.

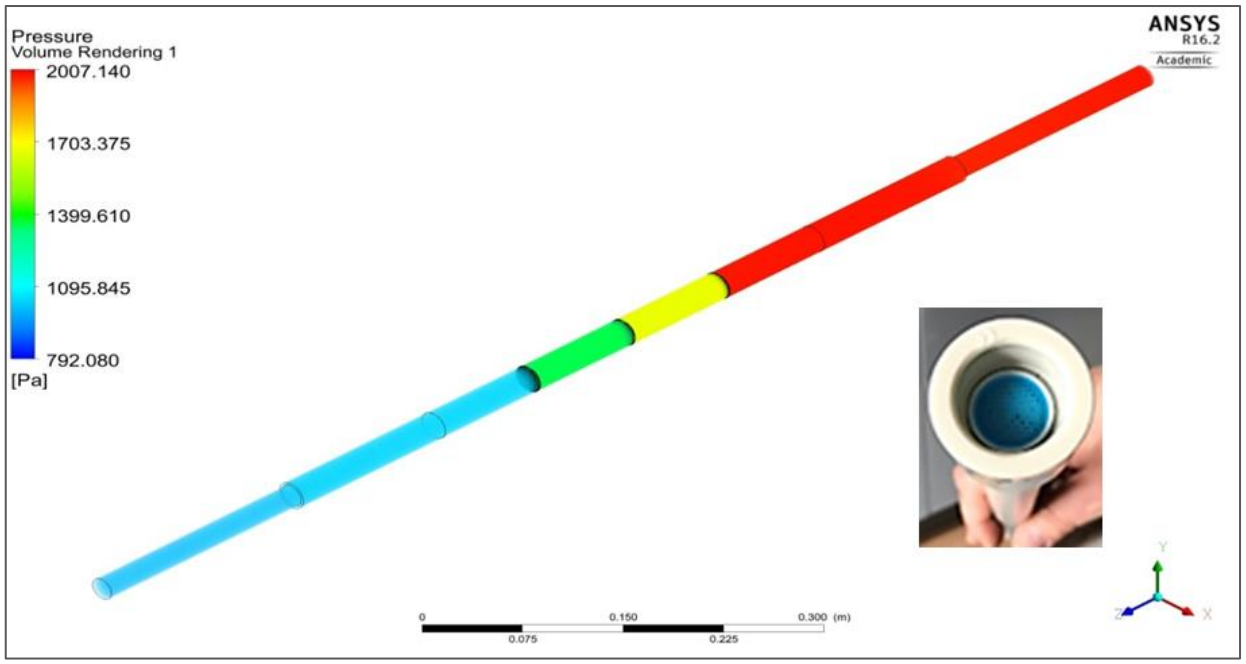

Figure 5 Simulation of the pressure field in experimental model No.2 for air flow 3820.03 l.h^{-1}

In Figure 5, the result of the flow simulation in Model No.2 for the air flow rate $q_{v,0}$= *3820.03 l.h^{-1}* from Table 3 in [15] is shown. The visual representation of the pressure field along the length of the measuring element is depicted using a colour contour. From the analysis of the pressure field, a stepwise pressure gradient can be observed at the locations of the siphon strainers. The filling of the measuring element creates local pressure resistances, which reduce the pressure only at the location of the siphon strainers.

In Figure 6, the stepwise pressure decrease along the length of the measuring element is shown using a curve, which indicates the locations of the siphon strainers. For the CFD software simulations, the geometry parameters corresponding to the shape of the screens and the openings in them were set.

From the analysis of the pressure profile along the length of the measuring element for the set flow rate and initial pressure, a pressure decrease of *1022 Pa* across the entire measuring element was obtained using CFD simulation. Each screen accounted for a pressure decrease of *304 Pa* for the simulated air flow.

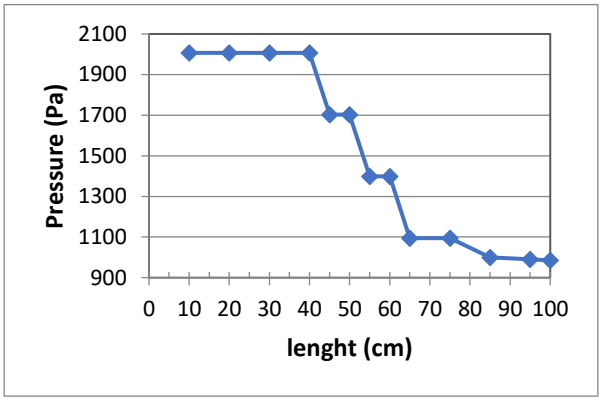

Figure 6 Pressure decrease along the length of the No.2 model for CFD flow simulation – Air

The conducted CFD simulation demonstrates the potential for reducing pressure based on the number of siphon strainers or local obstacles used. The graphical representation of the pressure decrease between the inserted screens shows no further pressure decrease, whereas a linear pressure decrease is observed at each screen. This analysis indicates that the thickness of the inserted screens also affects the pressure decrease. The pressure decrease at the end of the measuring element is caused by the change in geometry at the model's outlet.

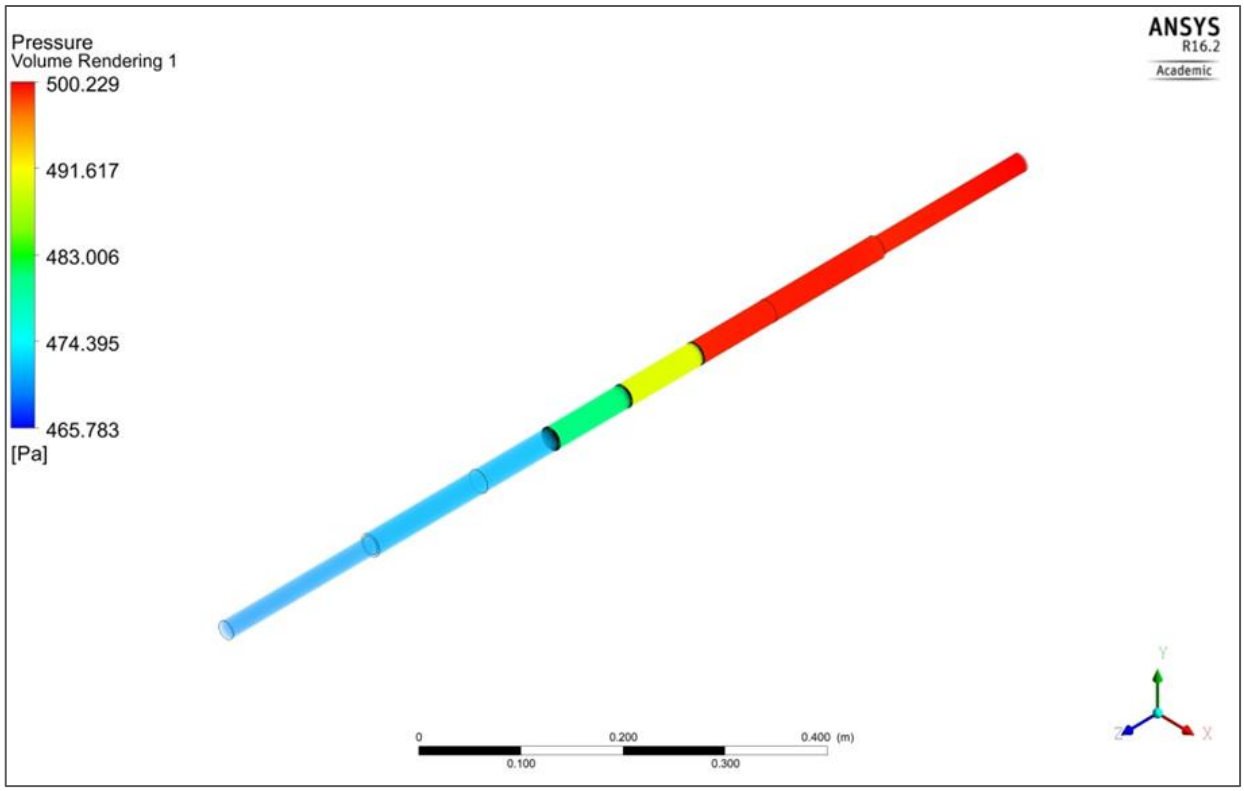

Figure 7 Simulation of the pressure field in experimental model No.2 for natural gas flow 1024.84 l.h^{-1}

In Figure 7, the result of the flow simulation in Model No.2 for the natural gas flow rate $q_{v,0}$*= 1029.84 l.h^{-1}* and input pressure *500 Pa* from Table 4 in [15] is shown. The visual representation of the pressure field along the length of the measuring element is depicted using a colour contour. From the analysis of the pressure field, a stepwise pressure decrease can also be observed at the locations of the siphon strainers.

In Figure 8, the stepwise pressure decrease along the length of the measuring element is shown using a curve, which indicates the locations of the siphon strainers. For the CFD software simulations, the created model and parameter settings for the geometry corresponding to the shape of the screens and the openings in them were used, as with the air flow.

From the analysis of the pressure profile along the length of the measuring element for the set flow rate and initial pressure, a pressure decrease of *36 Pa* across the entire measuring element was obtained using CFD simulation. Each screen accounted for a pressure decrease of *9 Pa* for the simulated air flow. Similar to the simulations for the natural gas flow in CFD model No.1, this case also shows the influence of the change in the medium used on the pressure decrease. The physical properties of natural gas significantly affect the flow characteristics and thus the pressure decrease in the measuring element. The pressure decrease after the last siphon screen is also influenced by the geometry at the outlet of the model.

The character of the flow is laminar along the length of the model due to the low flow of natural gas. The flow is only affected at the transitions through the siphon strainers, where flow lines are formed defined by the size and number of holes in the strainer. Similar to airflow, the magnitude of the pressure loss can only be influenced by the location, number and geometry of the siphon strainers.

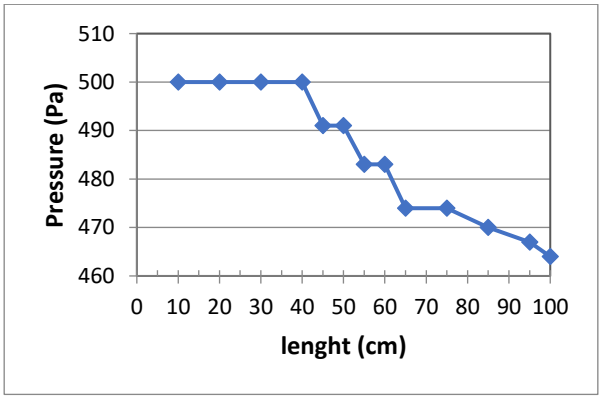

Figure 8 Pressure decrease along the length of the No.2 model for CFD flow simulation – Natural gas.

3.3 Experimental device No.3

The created CFD model No.3 was based on the experimental device described in [16]. In the simulation, one flow rate of the gaseous medium and the measured pressure at the beginning of the experimental device were set.

The next parameter was based on the fill formed by the capillaries, which formed a resistance to the flow and thus created a pressure gradient at the fill location.

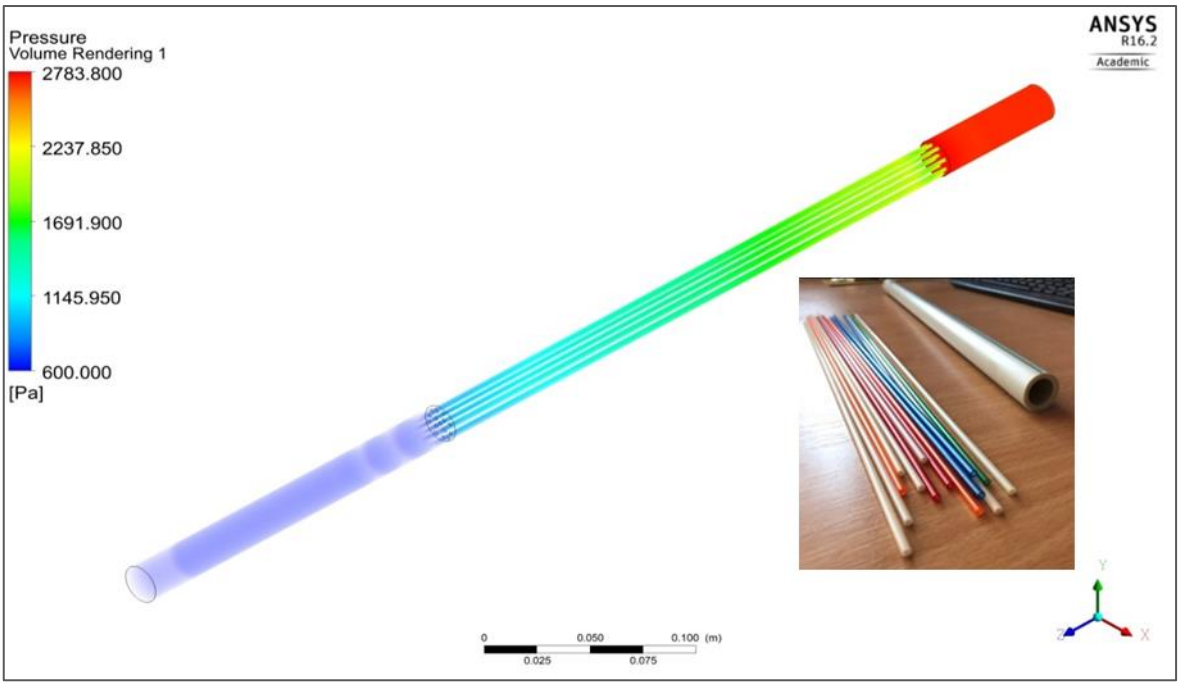

Figure 9 Simulation of the pressure field in experimental model No.3 for air flow 3150.37 l.h^{-1}

In Figure 9, the result of the flow simulation in Model No.3 for the air flow rate $q_{v,0}$= *3150.37 l.h^{-1}* and input pressure *2800 Pa*, which were obtained from experimental measurements and presented in [16]. The visual representation of the pressure field along the length of the measuring element is depicted using a colour contour. From the analysis of the pressure field, a smooth pressure decrease can be observed along the length of the model.

In Figure 10, the smooth pressure decrease along the length of the measuring element is shown using a curve, which indicates a more or less linear pressure decrease along the length of the inserted capillaries.

For the CFD software simulations, the geometry of the capillaries and the internal geometry of the measuring element were used. The linear arrangement of the capillaries inside the model changes the airflow characteristics and creates flow laminarization. The laminarization of the flow is achieved by dividing the total flow into partial volumes. The geometry and length of the capillaries create a pressure decrease due to the lengthwise pressure loss. Therefore, a stepwise pressure change cannot be observed in the measuring element of the capillary model.

From the analysis of the pressure profile along the length of the measuring element for the set flow rate and initial pressure, a pressure decrease of *2183 Pa* across the entire measuring element was obtained using CFD simulation. The initial significant pressure decrease is caused by the change in geometry at the inlet to the capillaries in the measuring element. The change in flow characteristics is due to the small diameters of the capillaries and the high resistance along the length of these capillaries, which also explains the flow laminarization.

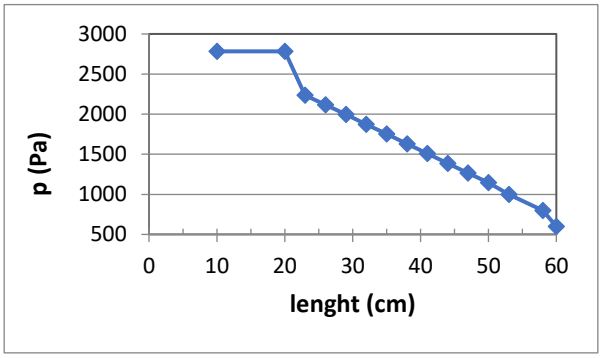

Figure 10 Pressure decrease along the length of the No.3 model for CFD flow simulation - Air

In Figure 10, it is clearly observable that the pressure loss is influenced only by the *40 cm* length of the filling made up of capillaries. Compared to Figure 9, it can be seen that the pressure no longer changes beyond the capillaries, and for measuring low flow rates, it is important to monitor only the pressure decrease in the filling made up of capillaries.

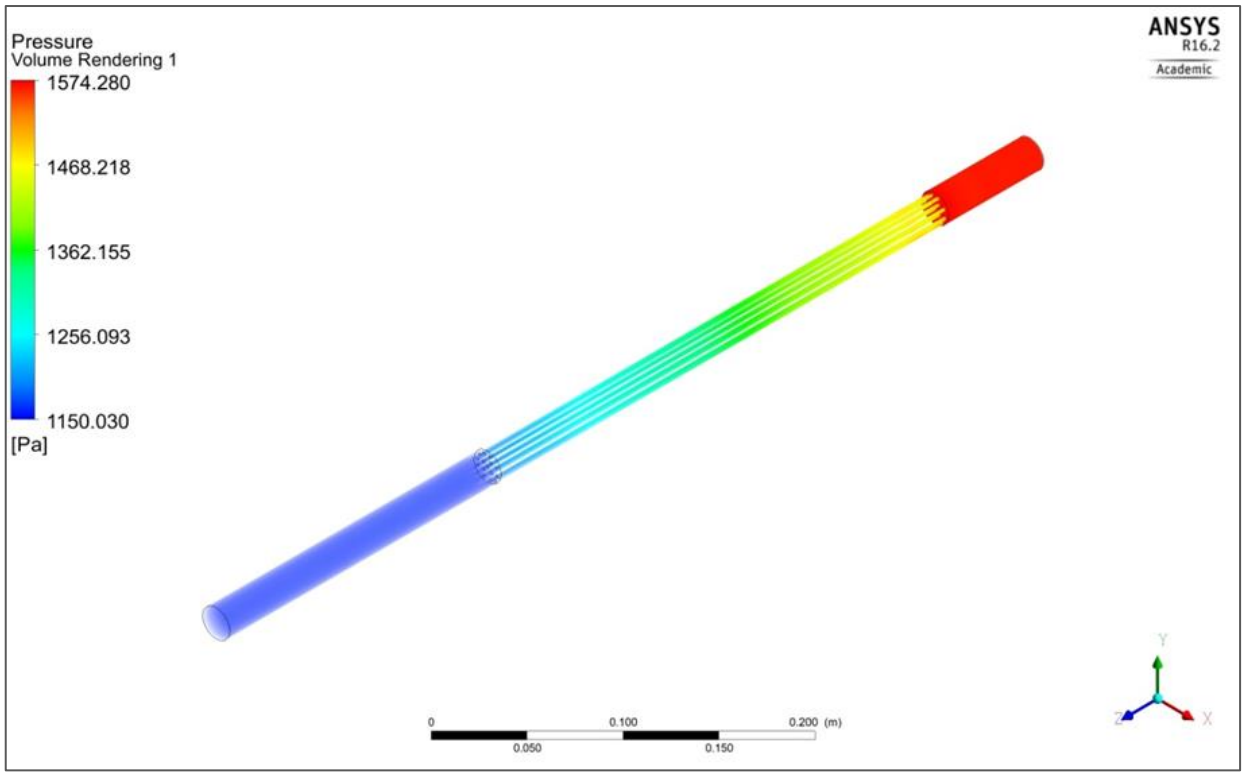

Figure 11 Simulation of the pressure field in experimental model No.3 for natural gas flow 1651.02 $l.h^{-1}$

In Figure 11, the result of the flow simulation in Model No.2 for the natural gas flow rate $q_{v,0}$*= 1651.02* $l.h^{-1}$ and input pressure *1574 Pa*, which were obtained from experimental measurements and presented in [16]. The visual representation of the pressure field along the length of the measuring element is depicted using a colour contour. From the analysis of the pressure field, a smooth pressure decrease can also be observed along the length of the model in this case.

In Figure 12, the smooth pressure decrease along the length of the measuring element is shown using a curve, which indicates a more or less linear pressure decrease along the length of the inserted capillaries. Here too, at the inlet to the capillaries, there is a significant pressure decrease caused by the redistribution of the main flow into smaller gas streams within the capillaries. This change can be characterized as a local pressure loss.

From the analysis of the pressure profile along the length of the measuring element for the set flow rate and initial pressure, a pressure decrease of *424 Pa* across the entire measuring element was obtained using CFD simulation. Similar to the airflow, no pressure decrease was recorded after the capillaries in the case of natural gas flow. Therefore, it can be inferred that the laminarization of the gas flow in the capillaries prevents further pressure decrease beyond the capillaries.

The actual measuring device, a Laminar Flow Element, operates with a pressure decrease measured across a single capillary. For simplification, the experimental device was based on the total pressure difference across the entire measuring element. As a result, while the principle was maintained, the measurement itself was simplified. The analysis of the simulation using the CFD model shows the influence of the inlet part on the pressure loss. However, when considering the total pressure difference, it is easier to use this to calculate the flow rate through the entire measuring element.

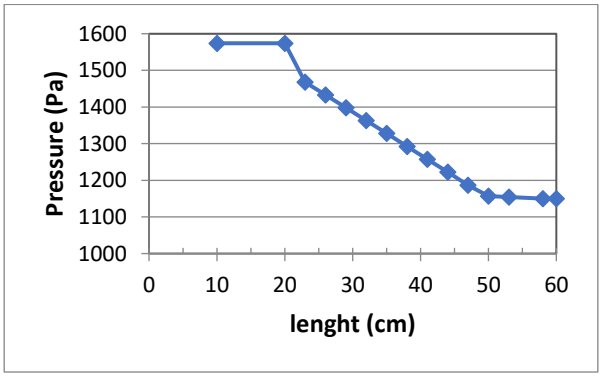

Figure 12 Pressure decrease along the length of the No.3 model for CFD flow simulation – Natural gas

The obtained simulation results suggest that through visualizations or simulations using the developed CFD models, it is possible to better design potential modifications to actual measuring devices. This finding also applies to alternative measuring devices designed based on fluid flow knowledge and commercially manufactured measuring devices. The analysis of the obtained results indicates a further path for designing and modifying similar models for fluid flow measurement.

4 Conclusion

The analysis of pressure losses using CFD modelling revealed the following:

1. Flow within experimental devices induces a pressure loss due to local obstructions and characteristic dimensions, specifically the internal geometry of the device.
2. Semipermeable obstructions, as observed in experimental device No.1, result in a gradual pressure decrease along the length of the semipermeable filler. Overall, only a minor pressure gradient can be achieved while maintaining laminar flow. The magnitude of the pressure gradient can be influenced by the quantity and density of the filler.
3. Local obstructions, as demonstrated in experimental device No.2, cause abrupt pressure changes, with the total decrease dependent on the number of these obstructions.
4. The filler in experimental device No.3, composed of capillaries, causes a gradual pressure to decrease along the length of the device. This pressure decrease is dependent on the number and diameters of the capillaries, as well as the length of the device and the capillaries within it.
5. Each experimental device can affect the pressure gradient and the laminarity of the flow depending on the properties of the flowing medium.

5 The reference list

[1] VARGA, A., JABLONSKÝ, G., LUKÁČ, L. KIZEK, J.: *Thermal technology for metallurgists* (In Slovak), 1.ed., Technical University in Košice, 2013.

[2] SVINOLOBOV, N.P., BROVKIN, V.L.: *Theoretical foundations of metallurgical heat technology*. Dnipro, Porogi, 2002.

[3] OVERMEEN, A.: Laminar flow vs Turbulent flow., Bronkhorst, [Online], Available: https://www.bronkhorst.com/int/blog-1/what-is-the-difference-between-laminar-flow-and-turbulent-flow/ [19 Dec 2023], 2023

[4] MIKAN, J.: *Gas measurement*. Říčany u Prahy: GAS s.r.o., 2003.

[5] RAJNIAK, I., ZAVODNOV, P., KUČÁK, Ľ.: *Measurement in thermal power engineering*. Bratislava, alfa, 1989.

[6] RAJNIAK, I., ZAVODNOV, P., KUČÁK, Ľ.: *Tepelno-energetické a emisné merania*. Bratislava, Ister Science, 1997.

[7] NUTIL, J., ČECH, V.: *Measurement in the metallurgical industry*. Praha, SNTL,1982.

[8] HALAJ, M., KUREKOVÁ, E.: Measurement of flow rate, overflow quantity (1). *AT&P journal, Princípy automatizáci*, No. 11, pp. 18-19, 2011.

[9] ĎAĎO, S. a kol. 2005. *Measurement of flow and height*. 3. vyd. Praha : Technická literatúra BEN, 2005.

[10] DORLAND, G.J.: Laminar flow element; a critical element for flow meters., Bronkhorst, [Online], Available: https://www.bronkhorst.com/int/blog-1/laminar-flow-element-a-critical-element-for-flow-meters/ [1 Feb 2022], 2022

[11] DEARBORN, U of M: *Meriam laminar flow element, Instruction manual*. Technical Note 2A, The Merian Instrument Co., Cleveland, Ohaio,1961.

[12] WRIGHT, J.D., COBU, T., BERG, R.F., MOLDOVER, M.R.: Calibration of Laminar Flow Meters for Process Gases. *Flow Measurement and Instrumentation*, Vol. 25, No. 6, pp. 8-14, 2012.

[13] LUKÁČ, P., HORBAJ, P., SEDLÁKOVÁ, J.: Options to Evaluate The Effects of a Change in the Shape of the Flow Cross-Section of a Ball Valve on Its Flow Control Properties. *Acta Mechanica Slovaca*, Vol. 18, No. 1, pp. 38-43, 2014.

[14] LUKÁČ, P.: *'Reducing the impact on flow measurement accuracy of ultrasonic flowmeters for gas transmission'*, in LAZIĆ, L. AND KIZEK, J. (ed.) *Selected Problems in the Transport of Natural Gas*, Zagreb, University of Zagreb Faculty of Metallurgy, 2017.

[15] POLIVKA, N., KIZEK, J., RIMÁR, M., VARGA, A., ROTH, J.: Experimental Devices for Measuring Small Gas Flows, *Advance in Thermal Processes and Energy Transformation*, Vol. 5, No. 3, pp. 45-54, 2022.

[16] HREBÍK, T., KIZEK, J., FEDÁK, M., VARGA, A., ROTH, J.: Experimental Device for the Measuring of Small Gas Flows Utilizing the Principal of Laminar Flow Elements, *Advance in Thermal Processes and Energy Transformation*, Vol. 6, No. 3, pp. 52-58, 2023.

[17] SPP-Distribucia: Natural gas composition and emission factor, [Online], Available: https://www.spp-distribucia.sk/dodavatelia/informacie/zlozenie-zemneho-plynu-a-emisny-faktor/ [20 Dec 2021], 2021.

Acknowledgement

This article was supported by the state grant agency for supporting research work and co-financing the project KEGA 024TUKE-4/2024.